



Tectonics

RESEARCH ARTICLE

10.1002/2014TC003561

Key Points:

- Fault geometry and geologic framework characterized within the SAF-CF junction
- Potential slip-transferring cross faults identified and characterized
- Discovered abundant serpentinite and related Coast Range Ophiolite in subsurface

Correspondence to:

J. T. Watt,
jwatt@usgs.gov

Citation:

Watt, J. T., D. A. Ponce, R. W. Graymer, R. C. Jachens, and R. W. Simpson (2014), Subsurface geometry of the San Andreas-Calaveras fault junction: Influence of serpentinite and the Coast Range Ophiolite, *Tectonics*, 33, 2025–2044, doi:10.1002/2014TC003561.

Received 20 FEB 2014

Accepted 22 SEP 2014

Accepted article online 23 SEP 2014

Published online 27 OCT 2014

Subsurface geometry of the San Andreas-Calaveras fault junction: Influence of serpentinite and the Coast Range Ophiolite

Janet T. Watt¹, David A. Ponce², Russell W. Graymer², Robert C. Jachens², and Robert W. Simpson²

¹U.S. Geological Survey, Santa Cruz, California, USA, ²U.S. Geological Survey, Menlo Park, California, USA

Abstract While an enormous amount of research has been focused on trying to understand the geologic history and neotectonics of the San Andreas-Calaveras fault (SAF-CF) junction, fundamental questions concerning fault geometry and mechanisms for slip transfer through the junction remain. We use potential-field, geologic, geodetic, and seismicity data to investigate the 3-D geologic framework of the SAF-CF junction and identify potential slip-transferring structures within the junction. Geophysical evidence suggests that the San Andreas and Calaveras fault zones dip away from each other within the northern portion of the junction, bounding a triangular-shaped wedge of crust in cross section. This wedge changes shape to the south as fault geometries change and fault activity shifts between fault strands, particularly along the Calaveras fault zone (CFZ). Potential-field modeling and relocated seismicity suggest that the Paicines and San Benito strands of the CFZ dip 65° to 70° NE and form the southwest boundary of a folded 1 to 3 km thick tabular body of Coast Range Ophiolite (CRO) within the Vallecitos syncline. We identify and characterize two steeply dipping, seismically active cross structures within the junction that are associated with serpentinite in the subsurface. The architecture of the SAF-CF junction presented in this study may help explain fault-normal motions currently observed in geodetic data and help constrain the seismic hazard. The abundance of serpentinite and related CRO in the subsurface is a significant discovery that not only helps constrain the geometry of structures but may also help explain fault behavior and the tectonic evolution of the SAF-CF junction.

1. Introduction

In the southern San Francisco Bay Area the San Andreas fault system transitions from a single creeping trace into two fault zones; the San Andreas fault zone (SAFZ) and the Calaveras fault zone (CFZ, Figure 1). The San Andreas-Calaveras fault (SAF-CF) junction represents a three-dimensional volume of crust that contains the principal San Andreas and Calaveras Faults, as well as secondary faults, including the Quaternary active Bear Valley, Bradford, Paicines, Pine Rock, San Benito, Tres Pinos, and Quien Sabe Faults. According to this definition, the SAF-CF junction is approximately 60 km long, from Hollister in the north to Bitterwater Valley in the south, and up to 17 km wide. The Paicines, San Benito, and Pine Rock Faults form the southern extension of the CFZ within the junction and, along with the SAFZ, are the focus of this study. At the surface, the San Andreas and Calaveras fault zones are both creeping [e.g., Galehouse and Lienkaemper, 2003; Titus et al., 2005] and parallel each other for about 50 km from Paicines to approximately 18 km south of San Benito, separated by only 2 to 6 km [U.S. Geological Survey and California Geological Survey, 2006]. The wedge of crust between the SAFZ and CFZ is variably deformed and characterized by a complicated network of anastomosing faults, both active and inactive.

Early mapping efforts within the junction recognized the steeply dipping nature of both the SAFZ and CFZ near Hollister. Geologic mapping and associated gravity analysis north of Paicines [Pavoni, 1973; Robbins, 1982] indicated NNE-SSW compression during the Plio-Pleistocene and a southwest dipping SAF within the upper 5 km that presumably steepened at depth. The southwest dip of the SAF was later confirmed by analysis of geology, gravity, magnetic, seismicity, magnetotelluric, and tomographic data [Dorbath et al., 1996; Langenheim et al., 1997; Thurber et al., 1997; Templeton et al., 2001; Bedrosian et al., 2002; Jachens et al., 2002; Jachens and Griscorn, 2004]. The dip of the SAF south of Bear Valley within the junction is not as well documented. Investigation of the density structure of the SAFZ near Bear Valley [Wang et al., 1986] revealed a vertical to steeply northeast dipping fault zone characterized by low-density material that extends to depths of 15 km. As earthquake relocation techniques improved, researchers noticed that the seismicity along the

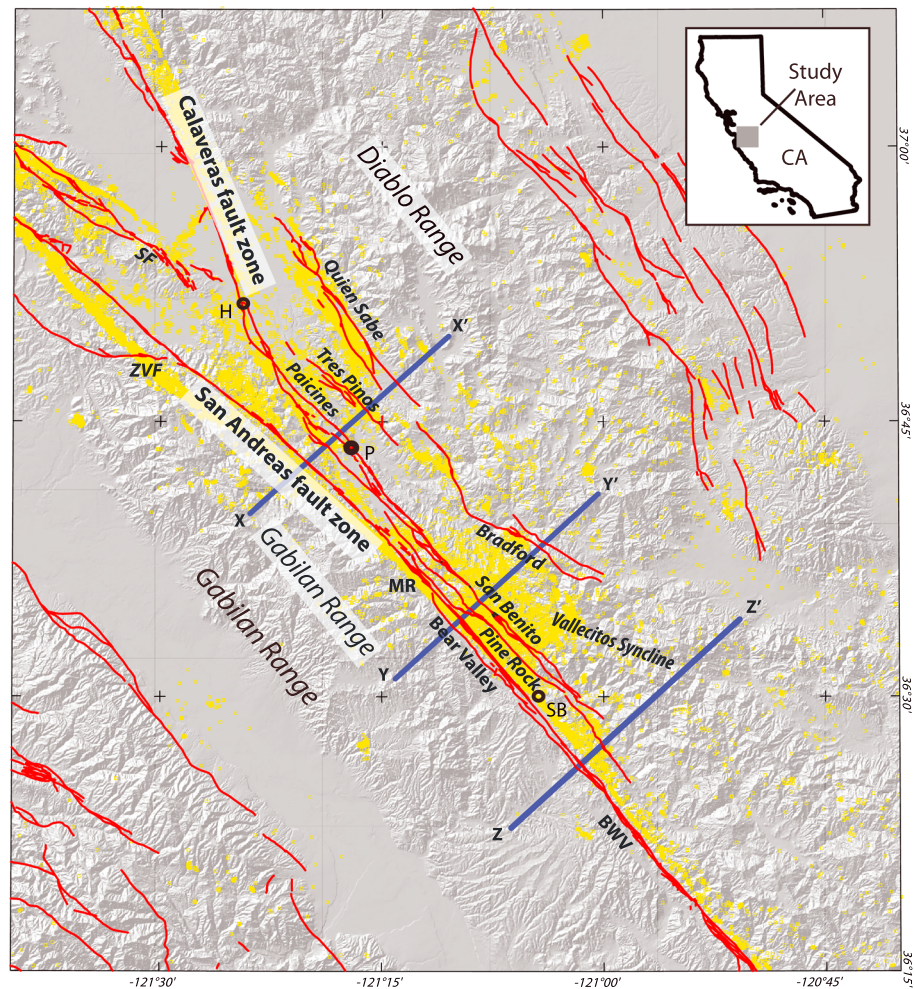


Figure 1. Topographic map of the San Andreas-Calaveras fault junction. Red lines, Quaternary active faults [U.S. Geological Survey and California Geological Survey, 2006]; yellow squares, relocated seismicity [Waldhauser and Schaff, 2008]; blue lines, geophysical model profiles; BWV, Bitterwater Valley; H, Hollister; P, Paicines; MR, Melendy Ranch; SB, San Benito; SF, Sargent Fault; and ZVF, Zayante-Vergeles Fault.

southern CFZ near Hollister was offset to the east of the surface trace. This offset was interpreted to represent a northeast dipping CFZ [Dorbath et al., 1996] and was supported by gravity and magnetic modeling [Jachens et al., 2002]. The geometry of the CFZ south of Hollister is not well constrained. The current geometry of the SAF-CF junction is not kinematically sustainable without deformation on additional fault surfaces or reorganization of the major faults in the region [Burford and Savage, 1972; Andrews, 1989]. Crustal deformation models involving vertical San Andreas and Calaveras Faults in the southern San Francisco Bay Area [Burgmann, 1997] do not fit geodetic observations of fault-normal motion and argue for the existence of nonvertical structures.

More than 170 km of right-lateral slip has been transferred through this fault intersection since 12 Ma when the SAF propagated to this area [McLaughlin et al., 1996; Jachens et al., 1998]. While the total offsets for both the San Andreas and Hayward-Calaveras Faults are well established [e.g., McLaughlin et al., 1996; Wakabayashi, 1999; Jachens and Zoback, 1999; Zoback et al., 1999; Graymer et al., 2002; Jachens et al., 2002], the three-dimensional fault geometry of the southern CFZ and other structures responsible for slip transfer through this important junction are poorly understood. There are no cross faults present in the surface geology of the SAF-CF junction that show evidence of accommodating the proposed 170 km of right-lateral offset. Integrated geological and geophysical studies of the Hayward-Calaveras fault zones have shown that there are often discrepancies between the surface manifestations of faults and the fault structure at

seismogenic depths [e.g., Michael, 1988; Ponce et al., 2004; Simpson et al., 2003; Graymer et al., 2007; Hardebeck et al., 2007; Watt et al., 2007, 2011], highlighting the importance of subsurface investigations in comprehensive characterization of fault zones. While previous studies have mainly focused on either one particular fault, or a small portion of the SAF-CF junction, we perform an integrated geological and geophysical investigation spanning the entire junction south of Hollister.

The recent occurrence of large ($M_w > 7$) multifault earthquakes highlights the need to evaluate the potential for through-going ruptures at fault junctions and to reassess the seismic hazard along faults that creep. Fault geometry and fault connectivity are key components of seismic hazard analysis at fault intersections because the three-dimensional geometry of faults affects the dynamics of fault rupture, slip, and ground motion [Oglesby et al., 2000]. While an enormous amount of research has been focused on trying to understand the geologic history and active tectonics of the SAF-CF junction, fundamental questions remain concerning fault geometry and mechanisms for slip transfer through the junction.

In this paper we address the question of how slip is transferred through the SAF-CF junction, a fault intersection in which slip is partitioned between two principle faults that do not directly connect at the surface. We take advantage of the recent advances in earthquake relocation techniques [e.g., Waldhauser and Ellsworth, 2002; Schaff et al., 2002; Hardebeck et al., 2007] and recent gravity and magnetic data to (1) investigate the geometry and three-dimensional geologic framework of the San Andreas-Calaveras fault junction and (2) identify potential slip-transferring structures within the junction. In light of these observations, we present a fault model that highlights previously unrecognized northeast dipping structures, buried cross faults, and an abundance of serpentinite and related Coast Range Ophiolite (CRO) in the subsurface. We discuss the implications of this model for fault development, fault behavior, and seismic hazard. Our results emphasize the importance of integrated geologic and geophysical studies in determining three-dimensional fault geometry and suggest that evaluation of fault connectivity based on surface data alone may result in an inaccurate assessment of the seismic hazard.

2. Geologic Setting

Within the study area, the SAF juxtaposes granitic and metamorphic basement rocks of the Gabilan Range with Franciscan Complex, Coast Range Ophiolite (CRO), and Great Valley sequence basement rocks of the Diablo Range. The Gabilan Range basement rocks are intruded by the Oligocene pinnacles volcanics and overlain by Neogene sedimentary rocks. The Mesozoic basement rocks of the Diablo Range are intruded by the Miocene Quien Sabe volcanics and overlain by Neogene sedimentary rocks, including the upper Miocene and Pliocene marine sandstones of the Etchegoin Formation.

The Vallecitos syncline is an important structure within the junction, not only as a prolific oil and gas province in central California but also because it records a history of deformation along the San Andreas transform margin since about 12–14 Ma, when the Mendocino triple junction reached this latitude. The WNW-ESE trending Vallecitos syncline formed during early stages of strike-slip faulting (about 12–14 Ma) as a result of distributed shear [Miller, 1998]. We provide evidence suggesting that the Vallecitos syncline bends into parallelism with the CFZ near San Benito and extends northward beneath Pliocene and younger deposits.

The wedge of crust between the San Andreas and Calaveras fault zones south of Hollister is characterized at the surface by variably deformed Miocene and younger sedimentary rocks overlying primarily Diablo Range basement rocks (Figure 2). Outcrops of Salinian granitic and metamorphic rocks occur in fault slices along the SAFZ, and faulted slivers of serpentinitized ultramafic rock and Jurassic to Cretaceous sedimentary rocks are mapped throughout the junction south of Paicines [Wagner et al., 2002; Dibblee and Minch, 2007a, 2007b, 2007c, 2007d, 2007e]. Serpentinitized ultramafic rocks within the SAF-CF junction are probably part of the CRO, which represents middle to upper Jurassic oceanic crust that formed in a forearc basin and consists of mainly serpentinite, gabbro, and basalt [Hopson et al., 1981]. The CRO forms the basement of the Great Valley sequence and is correlative and juxtaposed with the Franciscan Complex across the Coast Range Fault. The origin of the CRO and the timing and mechanism of tectonic emplacement of the unmetamorphosed CRO and overlying Great Valley sequence above the blueschist metamorphic rocks of the Franciscan Complex is still debated (see Dickinson et al. [1996] and Constenius et al. [2000], Figure 1 for a summary of tectonic models). Fragments of CRO have likely been brought to the surface by a combination of extensional, contractional, and transpressional tectonics [e.g., Wentworth et al., 1984; McLaughlin et al., 1988; Jayko et al.,

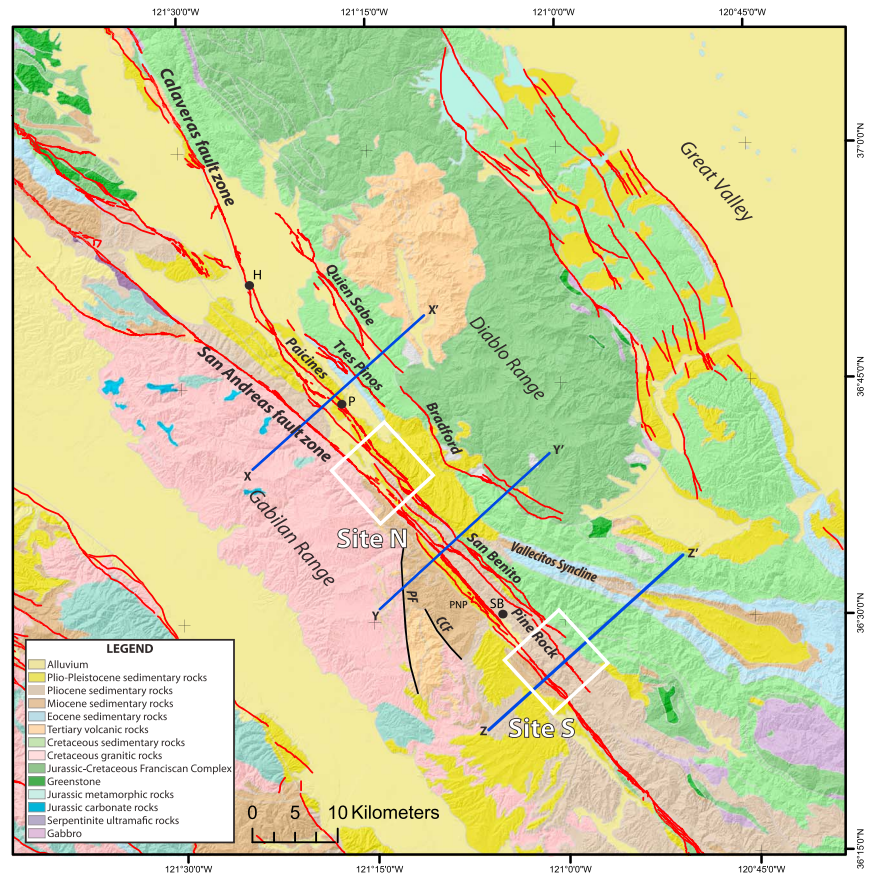


Figure 2. Simplified geologic map of the San Andreas-Calaveras fault junction (modified from Ludington *et al.* [2007]); CCF, Chalone Creek Fault; PF, Pinnacles Fault; and PNP, Pinnacles National Park; see Figure 1 for explanation.

1987; Wakabayashi and Unruh, 1995]. The ultramafic rocks within the junction are particularly important to this study because they are strongly magnetic and are surrounded by compositionally distinct, relatively nonmagnetic Gabilan granite and Franciscan mélangé, creating distinct magnetic gradients that can be modeled to understand the subsurface structure within the junction.

3. Methods

3.1. Relocated Seismicity

We used high-precision double-difference relocated seismicity (Figure 1) [Waldhauser and Schaff, 2008] recorded between 1984 and 2003 to define fault geometries and to identify and characterize potential slip-transferring structures within the SAF-CF junction, similar to the methods employed by Phelps *et al.* [2008] to map the Hayward and Calaveras Faults and Watt *et al.* [2011] to characterize the Mount Lewis fault zone. Details of the double-difference earthquake relocation method can be found in Waldhauser and Ellsworth [2000, 2002]. Cross sections of relocated seismicity spaced 2.5 km apart, oriented perpendicular to the fault junction, were generated for systematic analysis. Fault planes were identified by visual inspection of both the cross-sectional and map views of seismicity, and are shown by the colored boxes in Figure 5.

3.2. Geophysical Data

Gravity data for the study area were compiled and supplemented with new gravity stations within the SAF-CF junction and adjacent areas in the Diabolo Range (Figure 3a). Gravity data were processed using standard reduction techniques [Blakely, 1995] including topographic and isostatic corrections as described in Ponce *et al.* [2011]. Isostatic gravity anomalies reflect density changes within the middle to upper crust [Simpson *et al.*, 1986]. Gravity lows in the study area correspond to sedimentary basins such as the Hollister, Salinas,

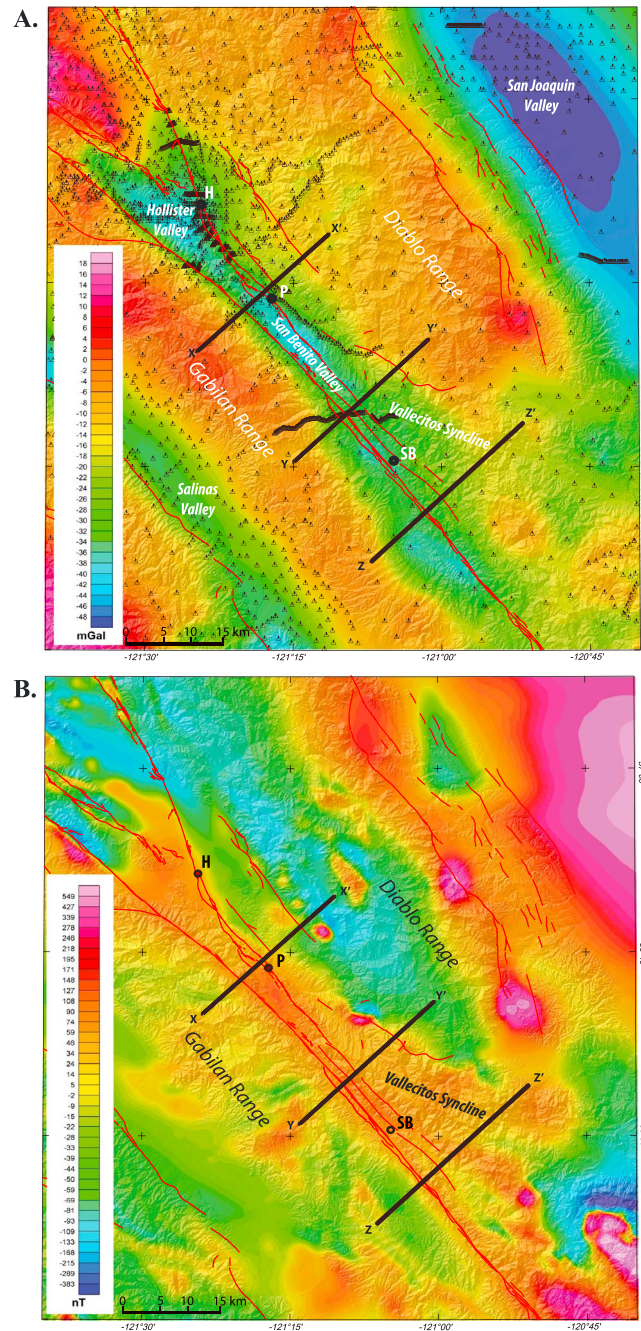


Figure 3. (a) Isostatic gravity map of the San Andreas-Calaveras fault junction. Black triangles, gravity station locations; black lines, geophysical model profiles; and (b) residual aeromagnetic map of the San Andreas-Calaveras fault junction. Black lines, geophysical model profiles; see Figure 1 for explanation.

San Benito, and San Joaquin Valleys. Gravity lows are also associated with thick deposits of Tertiary sedimentary rocks within the Vallecitos Syncline and within small basins west of the SAF. Prominent gravity highs coincide with outcrops of both granitic and Franciscan Complex basement rocks in the Gabilan and Diablo Ranges, respectively. Ophiolitic rocks, with the exception of serpentinite, are also associated with gravity highs, particularly along the eastern margin of the Diablo Range. The aeromagnetic data used in this study represent a mosaic of surveys that were flown at different times, flight line spacings, and flight line altitudes summarized in Roberts and Jachens [1999] and Langenheim [2014]. Data were reduced to total intensity magnetic field values and include corrections for diurnal variations of the Earth's magnetic field and removal of regional magnetic field of the Earth using an International Geomagnetic Reference Field model appropriate for the year of each survey. The residual magnetic anomalies shown in Figure 3b were analytically continued onto a common datum 305 m above the ground surface and merged into one seamless grid (500 m resolution). The magnetic highs (warm colors) represent rocks that contain magnetite, including mafic and ultramafic rocks of the Coast Range Ophiolite, mafic intrusive rocks in the Gabilan Range, and magnetic sedimentary rocks, such as the upper Miocene and Pliocene Etchegoin Formation [Perkins, 1987; Loomis, 1990]. In general, magnetic lows (cool colors) reflect relatively nonmagnetic alluvial fill, Franciscan Complex sedimentary rocks, the Great Valley sequence, and felsic igneous rock within the Gabilan Range. Of particular importance to this study are the anomalies associated with

strongly magnetic ophiolitic basement rocks, including serpentinite, and those associated with the weakly magnetic Etchegoin sedimentary rocks.

To identify potential cross structures within the SAF-CF junction, magnetic data were filtered and maximum horizontal gradients were calculated. To isolate magnetic anomalies within the shallow subsurface, the magnetic data were upward continued to a surface 50 m above the original flight path and then subtracted from the original magnetic grid (Figure 4). Because abrupt lateral changes (gradients) in the magnetization of

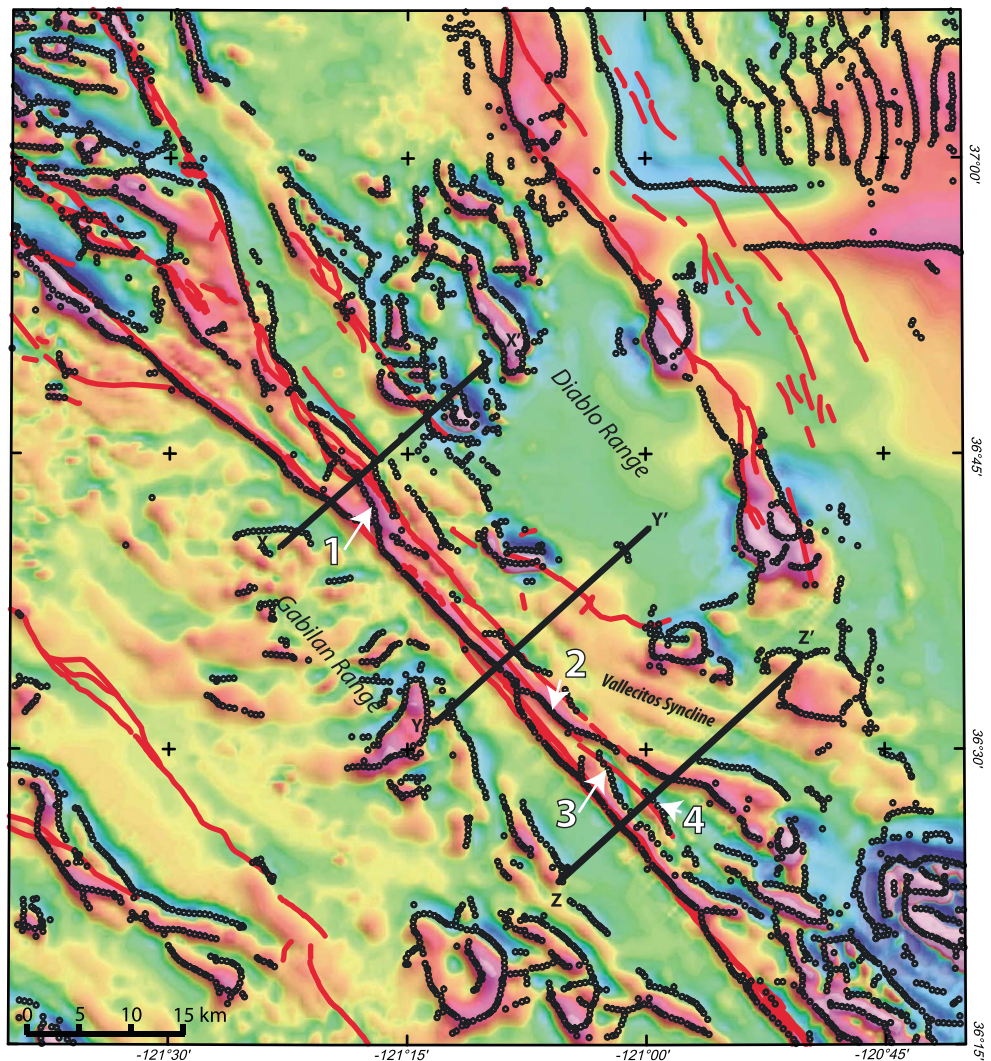


Figure 4. Filtered aeromagnetic map of the San Andreas-Calaveras fault junction. Black circles, locations of maximum horizontal gradients in the magnetic data; see Figure 1 for explanation.

rock units may represent lithologic or structural boundaries, maximum horizontal gradients of the filtered magnetic data were generated [Cordell and Grauch, 1983; Blakely and Simpson, 1986] to identify magnetic boundaries that may correspond to fault structures (Figure 4).

3.3. Geophysical Modeling

Two-dimensional gravity and magnetic modeling across the SAF-CF junction helps define the three-dimensional geologic framework of the junction, and in particular, constrains the geometry of structures within and adjacent to the junction. Gravity and magnetic data described above were used to model the density and magnetic property distributions associated with subsurface geologic features along model profiles X–Z (Figures 3a and 3b). Model profile locations were selected to target magnetic anomaly gradients along key fault structures and areas where the slip rate along the SAF appears to decrease. Although potential-field modeling inherently yields nonunique solutions [e.g., Blakely, 1995; Saltus and Blakely, 2011], the final models are geologically reasonable with minimal structural complexities and are based on numerous iterations using independent constraints, such as surficial geology [Wagner et al., 2002; Dibblee and Minch, 2007a, 2007b, 2007c, 2007d, 2007e; Ludington et al., 2007], seismic reflection data [Feng and McEvilly, 1983], and drill-hole data (Table 1). Rock properties are based on regional [Jachens et al., 1995] and local [Robbins, 1982; Ponce et al., 2003] representative densities and magnetic susceptibilities. Combined, these

Table 1. Well Information Used to Constrain Geophysical Models^a

Well	API	Operator	TD (m)	Age of Rock at Bottom
W1	6900031	TEPI	2360	mid-Pliocene
W2	6900219	D.D. Feldman Oil and Gas	1567	mid-Miocene
W3	6900279	Chevron	703	Cretaceous

^aTD, total depth of well in meters.

geologic, seismic, drill hole, and physical property constraints limit the inherent ambiguity and nonuniqueness of the resultant models.

When modeling geologic features within the upper crust, one must account for the effects of long-wavelength anomalies within the magnetic data caused by sources in the middle to lower crust. While the model results presented here are focused on the seismogenic crust within the junction, we expanded our modeling space well beyond the boundaries of our area of interest to include the long-wavelength anomalies evident in the regional magnetic data. The most significant regional magnetic anomaly within our study area reflects the westward extension of the magnetic basement (CRO) of the forearc deposits of the Great Valley sequence. Modeling of the magnetic field in central California indicates that the top of this magnetic basement slopes westward beneath the Franciscan Complex, reaching depths of 15 km or more below the SAF-CF junction [Jachens *et al.*, 1995; Ponce *et al.*, 2003]. To account for this particular long-wavelength anomaly, all of the models presented here include a deep, westward thinning magnetic body that terminates at the SAFZ (see Figure 7b).

4. Results

4.1. Fault Geometry From Seismicity

Map view and cross-sectional analysis of relocated seismicity help constrain fault geometry between approximately 2 and 12 km depth for seismically active structures within and adjacent to the SAF-CF junction, including the San Andreas, Calaveras, Paicines, Pine Rock, San Benito, Tres Pinos, and Quien Sabe Faults. The main trace of the SAFZ is clearly visible in cross sections of relocated seismicity as a vertical to steeply dipping structure between 5 and 10 km depth throughout the junction (Figure 5). Near Hollister, the SAF dips steeply to the southwest (about 70° to 80°, profile A-A', Figure 5). The southwest dip defined by seismicity is consistent with NNE-SSW compressional deformation evident within Pliocene and Pleistocene deposits east of the SAF [Rogers, 1993; Wagner *et al.*, 2002]. As the San Andreas and Calaveras fault zones bend into parallelism near Paicines, the dip of the SAFZ, as defined by seismicity, steepens to near vertical (profile D-D', Figure 5).

While seismicity cross sections show that the SAFZ remains vertical to steeply dipping throughout the junction, the fault plane defined by seismicity is offset up to 1 km from the surface trace. This offset is not consistent throughout the junction in either magnitude or direction, with an offset of about 1 km to the southwest near Paicines, no offset about 13 km north of the entrance to Pinnacles National Park, and about 1 km offset to the northeast near San Benito. This offset is the topic of a long-standing scientific debate and is thought to be produced by either fault dip [e.g., Thurber *et al.*, 1997] or by the velocity contrast across the fault [e.g., Ellsworth, 1975]. In our analysis, we do not attempt to apply any systematic shift to the hypocenters, but rather focus on the distribution of relative locations for defining fault planes.

Unlike the SAFZ, seismicity patterns along the CFZ in the northern portion of the junction are often diffuse and hypocenters do not consistently collapse onto easily identifiable fault planes. Where fault planes are visible in cross section, the CFZ dips moderately to steeply to the northeast. North of Hollister, along profile A-A' (Figure 5), the CFZ dips 70° to 80° to the northeast. Between profile B-B' and H-H' hypocenters do not collapse onto a clear Calaveras fault plane. Between profiles G-G' and J-J', a distinct wedge of seismicity is present within the junction that is bounded on the west by a near-vertical SAFZ and on the east by a northeast dipping (about 65°) structure. Interpreted fault planes bounding the northeastern edge of this wedge of seismicity intersect the surface at or very near the surface trace of the San Benito strand of the CFZ, suggesting that a northeast dipping CFZ bounds this seismically active wedge of crust. This area of the junction corresponds to the location of the Bear Valley earthquake sequence of 1972 (Figure 5), described by Ellsworth [1975] as occurring along the SAFZ and on cross faults between the San Andreas and Calaveras fault

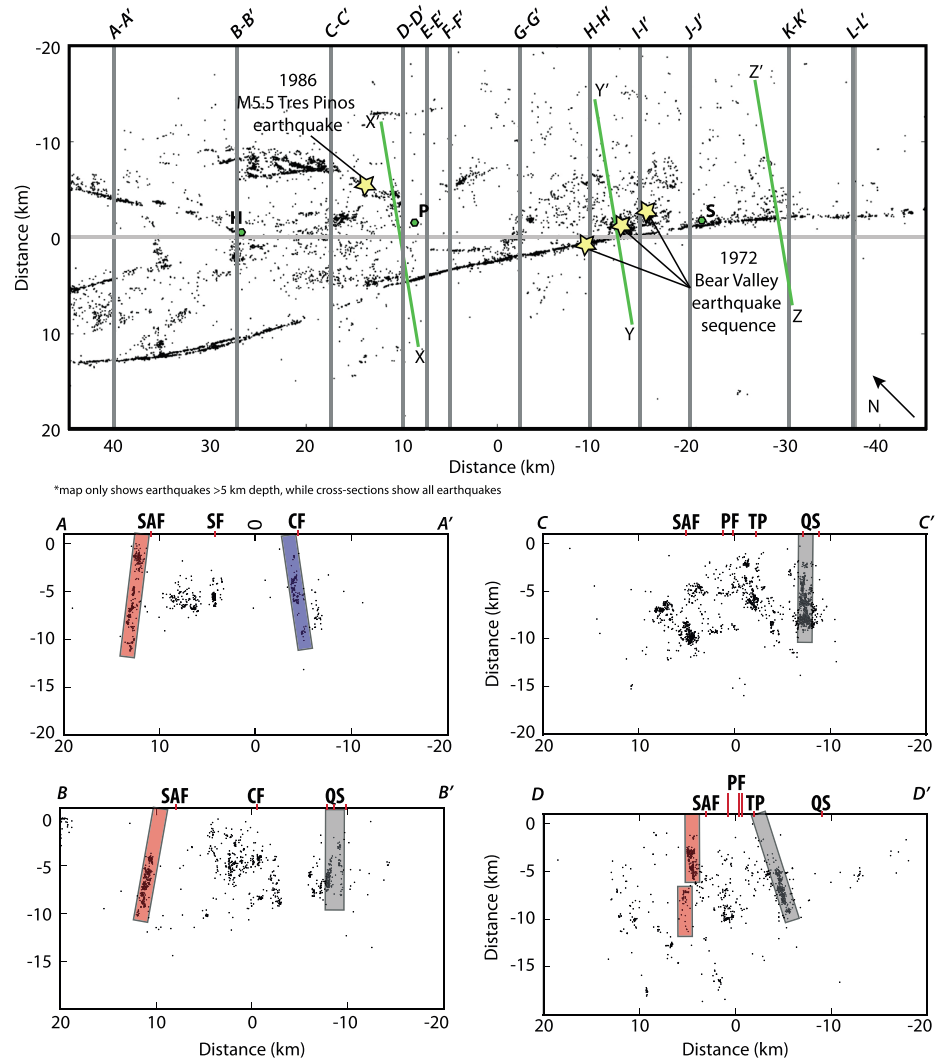


Figure 5. Map view of the San Andreas-Calaveras fault junction showing relocated seismicity (black dots) and locations of cross-sections AA'-LL' (grey lines). Note that the fault map only shows earthquakes below 5 km, while the cross-section profiles show all earthquakes. Red lines, quaternary active faults [U.S. Geological Survey and California Geological Survey, 2006]; green lines, locations of geophysical model profiles; red ticks along top of seismicity profiles, fault traces; interpreted fault plane associated with the San Andreas Fault (SAF) is highlighted in red, Calaveras Fault (CF) in blue; Quien Sabe (QS) and Tres Pinos (TP) Faults in grey; San Benito Fault (SBF) in green; and proposed cross faults in yellow. BF, Bradford Fault; BVF, Bear Valley Fault; CF, Calaveras Fault; PRF, Pine Rock Fault; QS, Quien Sabe Fault; SBF, San Benito Fault; SF, Sargent Fault; SAF, San Andreas Fault; and TP, Tres Pinos Fault.

zones. South of the intersection of the Vallecitos syncline, the wedge of seismicity within the junction disappears (e.g., profile K-K', Figure 5) and there is evidence that seismic activity shifts southwestward from the San Benito Fault and related northeast dipping structures to the southwest dipping Pine Rock Fault between profiles J-J' and K-K'. Seismicity profiles K-K' and L-L' show the Pine Rock Fault as a southwest dipping (80°) structure that intersects the SAFZ between 5 and 10 km depth (Figure 5).

4.2. Potential Slip-Transferring Structures

Using slip rates from alignment array data [Burford and Harsh, 1980], we identify zones with relatively large decreases in slip rate (going northward) along the SAFZ. A large decrease in slip rate may signal a transfer of slip from the SAFZ to the CFZ on a connecting structure. Two locations within the SAF-CF junction exhibit large changes in slip rate relative to adjacent areas; one in the northern part of the junction (site N, Figure 2) and one near the southern end of the join (site S, Figure 2). Sites N and S represent areas where the average slip rate

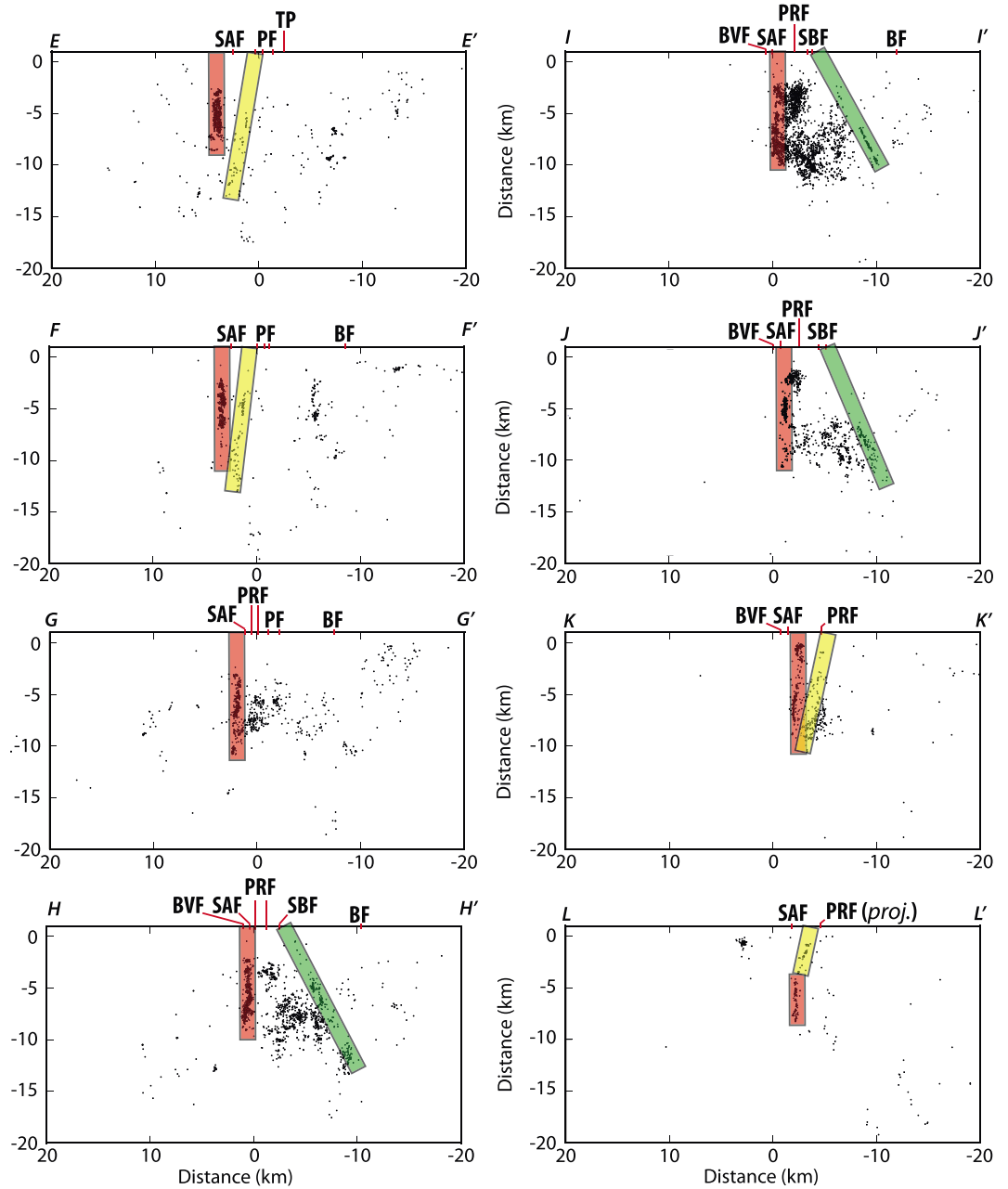


Figure 5. (continued)

decreased from south to north by 6 and 10 mm/yr, respectively. These results provided targets for more in-depth analysis, including detailed geophysical modeling, to identify and characterize buried cross faults.

Evaluation of both the map view and cross-sectional distribution of relocated seismicity within the junction highlights two fault planes that appear to branch off the SAFZ toward the CFZ. These fault planes coincide with slip rate decreases along the SAFZ (sites N and S), suggesting that these faults represent active structures that could transfer slip between the San Andreas and Calaveras fault zones. Near site N, seismicity profile F-F' (Figure 5) shows a southwest dipping alignment of hypocenters that intersects the SAFZ between 10 and 15 km depth. In map view (Figures 1 and 5), this fault plane is visible as a NNW-SSE alignment of epicenters that branches off of the SAFZ at an angle of about 10° to 15° toward the Paicines Fault. Southernmost seismicity profiles K-K' and L-L' (Figure 5), located near site S, show a southwest dipping alignment of hypocenters that

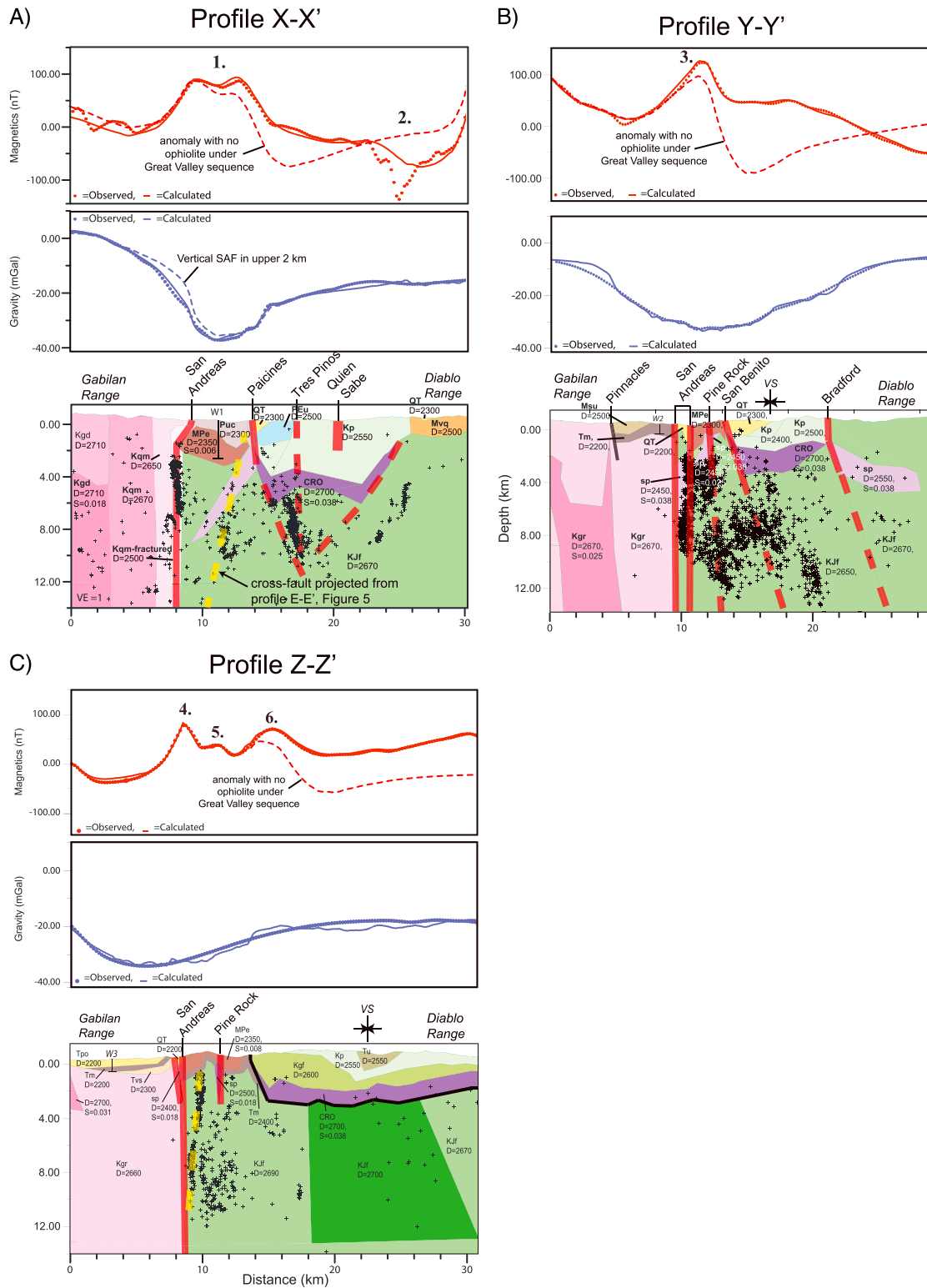


Figure 6. (a–c) Two-dimensional geophysical models along profiles X, Y, and Z (Figure 1). Black lines, faults; red lines, active or possibly active faults (dashed where inferred); yellow dashed lines, location of interpreted cross fault from Figure 5; D, density (kg/m^3); S, magnetic susceptibility (SI); plus, relocated seismicity [Waldhauser and Schaff, 2008]. Great Valley sequence includes Kgf, Gravelly Flat Formation and Kp, Panoche Formation. CRO, Coast Range Ophiolite; Kgr, granitic rocks; KJf, Franciscan Complex; Kqd, quartz diorite; Kqm, quartz monzonite; Tm, Monterey Formation; MPE, Etchegoin Formation; Msu, Miocene sedimentary rocks; MVq, Quien Sabe volcanics; PEu, Paleocene-Eocene sedimentary units; Puc, Pliocene sedimentary rocks; Q, Quaternary alluvium; QT, Plio-Pleistocene sedimentary rocks; sp, serpentinite; Tu, Tertiary sedimentary rocks; and Tsg, terrestrial conglomerate; Tpo, Pancho Rico Formation; Tvs, Vaqueros Sandstone; and VS, Vallecitos syncline.

projects toward the Pine Rock Fault and intersects the SAFZ at about 5 to 10 km depth. Again, this apparent shift in seismic activity from predominantly northeast dipping structures to the southwest dipping Pine Rock Fault coincides with the intersection of the Vallecitos syncline, suggesting that this impinging structure is directly influencing the geometry and active deformation within the junction.

Maximum horizontal gradients in shallow-filtered aeromagnetic data (Figure 4) illuminate four distinct gradient lineations (labeled 1–4, Figure 4) where structures may connect the San Andreas and Calaveras fault zones. Near site N there is a NNW-SSE-trending magnetic gradient (gradient 1, Figure 4) within the SAF-CF junction that is coincident with a southwest dipping seismicity lineation (profile F-F', Figure 5). Geophysical modeling along profile X-X' (Figure 6a) suggests that this gradient is associated with folding within the buried Etchegoin Formation and a sliver of serpentinite that is truncated along the Paicines Fault. Between sites N and S and geophysical model profiles Y-Y' and Z-Z' (Figures 6b and 6c) there is another NW-SE-trending gradient that crosses the junction (gradient 2, Figure 5) that corresponds to an area where serpentinitized ultramafic rock is mapped at the surface along both the Pine Rock and San Benito strands of the CFZ [Wagner *et al.*, 2002]. Coincident with site S there are two parallel NNW-SSE-trending magnetic gradients within the junction (gradients 3 and 4, Figure 4). Gradient 3 is coincident with a southwest dipping alignment of hypocenters that projects toward the surface trace of the Pine Rock Fault and intersects the SAFZ between 8 and 10 km depth (profiles K-K' and L-L', Figure 5). Gradient 3 is located between the SAFZ and CFZ and is likely associated with folding and faulting of the Etchegoin Formation (model Z-Z', Figure 6c). Gradient 4 occurs along the mapped trace of the Pine Rock Fault, where lenses of serpentinite are mapped along the southern margin of the fault [Dibblee and Minch, 2007d]. Geophysical model profiles X-X' and Z-Z' help further characterize gradients 1, 3, and 4. Concurrent analysis of relocated seismicity and shallow magnetic gradients suggests the existence of multiple subsurface structures, some coincide with sites N and S, that may transfer slip within the SAF-CF junction. All but one of these cross structures is associated with a fault-bounded sliver of serpentinitized ultramafic rock.

5. Discussion

5.1. Geophysical Models

Results of the 2-D geophysical modeling are discussed below, with each profile described in detail, including an integrated discussion of results presented above (Figures 6a–6c).

5.1.1. Model X-X'

A geophysical model along profile X-X' is in the northern portion of the SAF-CF junction and crosses the San Andreas, Paicines, Tres Pinos, and Quien Sabe Faults, all of which are seismically active Quaternary structures (Figure 6a). This model extends from the Gabilan Range, through the SAF-CF junction, crossing the Quien Sabe Fault and associated volcanic units, to the eastern side of the Diablo Range along the margin of the San Joaquin Valley. Model X-X' corresponds to an area where a cross structure between the San Andreas and Paicines Faults is proposed based on boundary analysis of filtered magnetic data.

Along this profile, both the San Andreas and Paicines Faults are associated with anomalies in the potential-field data. Geophysical modeling along profile X-X' suggests that the SAFZ has a relatively shallow dip of 55° to 60° in the upper 2 km, but quickly steepens to near vertical, which is consistent with previous modeling results [Pavoni, 1973; Langenheim *et al.*, 1997]. Model X-X' shows the mismatch of the gravity gradient with a vertical SAFZ. A southwest dipping SAF in the upper 2 km that steepens at depth provides the best fit to the observed gravity data and aligns the relocated seismicity with the fault at depth. In our model, moderately dense granitic rocks line the southwest side of the fault and at the surface are thrust over lower density Miocene and Pliocene sedimentary rocks mapped northeast of the fault zone [Wagner *et al.*, 2002]. Tectonic deformation of Pliocene and Pleistocene sediments east of the SAFZ [Pavoni, 1973; Wagner *et al.*, 2002] is consistent with NNE-SSW compression and reverse faulting in the near surface.

Along this profile, the Paicines Fault separates Eocene and younger sedimentary rocks on the northeast from Miocene and younger sedimentary rocks on the southwest. Diablo Range basement rocks are present on both sides of the fault at depth. The Paicines Fault is associated with a step-like feature in the gravity anomaly that likely reflects a change in sedimentary basin thickness across the fault, with thicker sediments to the southwest. There is a double-peaked magnetic anomaly (anomaly 1, Figure 6a) centered over the SAF-CF junction, with a magnetic gradient (Figure 4) corresponding to the surface trace of the Paicines Fault. We have

modeled this anomaly as resulting from three distinct magnetic bodies within the upper 8 km of the crust: (1) a 1 to 3 km thick layer of weakly magnetic Etchegoin Formation underlying the nonmagnetic Pliocene mudstone that is mapped at the surface by *Wagner et al.* [2002], (2) a southwest dipping, low density, sliver of serpentinite extending from 2 to 10 km depth between the Paicines and San Andreas Faults, and (3) a northeast dipping slice of dense ophiolitic rock extending from 2 to 6 km depth along a northeast dipping Paicines Fault. A minimum thickness of the Tertiary sedimentary deposits within the junction, including the Etchegoin Formation is constrained by gravity data and well information (W1, Figure 6a; Table 1). Modeling confirms the existence of a buried magnetic body within the SAF-CF junction that was suggested by our magnetic gradient analysis described above. This southwest dipping sliver of serpentinite between the San Andreas and Paicines Faults is associated with and forms an upward bound to a cluster of seismicity within the junction. The cross fault identified along seismicity cross-sections E-E' and F-F' (Figure 5) projects to this modeled serpentinite sliver (Figure 6a), suggesting structures bounding this serpentinite body may be actively transferring slip between the San Andreas and Paicines Faults in this area.

The serpentinitized ultramafic rock in these and subsequent models represents the base of the CRO. In our models, the CRO is represented either by isolated fault slivers of low-density serpentinite or by undivided CRO, which may include serpentinite. Along the Paicines Fault, the undivided CRO forms the basement of the Panoche Formation (upper Great Valley sequence equivalent rocks), and overlies Franciscan Complex rocks within what we interpret to be the northern extension of the Vallecitos syncline. This interpretation is supported by geologic mapping along profile X-X'. For instance, along the southwest margin of the Diablo Range, a thin lens of serpentinite is mapped at the surface in contact with southwest dipping beds of Panoche Formation to the southwest and Franciscan mélangé (KJf, Figure 6a) and overlying Quien Sabe Volcanics (Mvqa) to the northeast [*Wagner et al.*, 2002]. In our model, magnetic ophiolitic rocks project toward the surface along the northeast limb of the Vallecitos syncline; however, we are unable to resolve the geometry and depth extent of this magnetic feature because of an out-of-plane magnetic low (anomaly 2, Figure 6a) associated with highly magnetic gabbroic rocks outcropping just south of the profile [*Wagner et al.*, 2002].

Profile X-X' also crosses both the Tres Pinos and Quien Sabe Faults. Along this profile, the Quien Sabe Fault is not expressed in the potential-field data and has no associated seismicity. The Tres Pinos Fault runs along Tres Pinos creek and juxtaposes Paleocene to Eocene sedimentary rocks on the northeast with Plio-Pleistocene deposits on the southwest [*Wagner et al.*, 2002]. The surface trace of the Tres Pinos Fault is associated with a magnetic gradient (Figure 4) that, in model X-X', occurs where there is an inflection (fold) in the buried CRO. As described previously, the Tres Pinos Fault is associated with a northeast dipping alignment of hypocenters, suggesting the fault may accommodate oblique motion.

5.1.2. Model Y-Y'

Model profile Y-Y' crosses the SAF-CF junction about 5 km north of the entrance to Pinnacles National Park in Bear Valley (Figure 2). In this area the fault junction is about 4 km wide and is composed of numerous fault strands (Figure 1). Here the SAFZ is characterized by a main eastern strand and a western strand, the Bear Valley Fault. The Bear Valley Fault separates granitic basement rocks and overlying sedimentary and volcanic units on the west from Diablo Range basement rocks and overlying sedimentary units to the east within the junction. The CFZ includes two strands, the western Pine Rock Fault and the eastern San Benito Fault. The San Benito Fault separates Miocene and younger sedimentary rocks within the junction from Cretaceous and younger sedimentary rocks within the Vallecitos and Paicines synclines to the east. The Vallecitos syncline is a prominent WNW-ESE trending synclinal fold within the Diablo Range that intersects the CFZ in this area.

Along profile Y-Y' the SAF-CF junction is associated with a prominent (75 nT) magnetic high (anomaly 3, Figure 6b). Geologic mapping and geophysical modeling suggest that this anomaly is caused by bodies of serpentinite caught up in the fault junction. A sliver of serpentinite (sp, Figure 6b) is mapped at the surface between the Pine Rock and San Andreas Faults [*Wagner et al.*, 2002]. The northeast boundary of anomaly 3 is defined by a northeast dipping (about 70°) sliver of ophiolite that, if projected toward the surface, intersects the surface trace of the San Benito Fault. Therefore, we suggest this sliver of ophiolite is bounded by the CFZ. This steeply dipping ophiolite body flattens at about 4 km depth, forming the base of the Great Valley sequence within the Vallecitos syncline, similar to profile X-X'. While ophiolitic rocks along this profile are not mapped at the surface in contact with the Great Valley sequence, there are serpentinitized ultramafic rocks mapped in contact with Great Valley sequence rocks nearby along both limbs of the Vallecitos syncline

[Wagner *et al.*, 2002]. Significant model mismatch occurs if the CRO is defined as an isolated steeply dipping body along the CFZ, rather than extending beneath the syncline.

The Bear Valley section of the SAFZ is characterized by a wedge of scattered seismicity that is distributed between the San Andreas and Calaveras fault zones and is associated with the Bear Valley earthquake sequence of 1972 (as described above). Along profile Y-Y' the seismicity extends from the Bear Valley Fault on the southwest through the junction, continuing underneath the Vallecitos syncline to the northeast. Although individual fault planes are difficult to identify along this profile, concentrated seismicity appears to be associated with the edges of modeled serpentinite bodies within the junction, suggesting a link between serpentinite and active fault slip within the junction.

5.1.3. Model Z-Z'

Model profile Z-Z' crosses the southern portion of the SAF-CF junction about 10 km southeast of the town of San Benito (Figure 2). Here the SAFZ is about 500 m wide with two active strands, a western strand and the main eastern strand, that separate Gabilan Range granitic basement to the west from basement rocks of the Diablo Range to the east (Figure 6c). Along this profile, the Pine Rock Fault represents the southernmost extension of the CFZ. Modeling confirms the existence of a southwest dipping buried cross fault between the San Andreas and Pine Rock Faults inferred from integrated analysis of alignment array, seismicity, and aeromagnetic data. Along profile Z-Z', the Vallecitos syncline is just beginning to impinge on the SAF-CF junction and the unnamed fault along the southwestern limb of the syncline is not an active structure (Figure 6c).

Analysis of the magnetic data shows that both the San Andreas and Pine Rock Faults are associated with magnetic gradients (Figure 4), suggesting these faults bound magnetic bodies. Geophysical modeling along profile Z-Z' supports this association. The SAFZ is modeled as a vertical structure that is bounded by a sliver of serpentinite caught between traces of the fault within the upper 3 km. The magnetic gradient along the SAFZ in Figure 4 corresponds to the southwest edge of this serpentinite body and the western strand of the SAFZ. Below 3 km, the dip of the SAFZ can be modeled as either vertical or steeply northeast dipping. The Pine Rock Fault is modeled as a vertical fault to 3 km depth that is bounded to the southwest by a thin slice of serpentinite. Geologic mapping [Dibblee and Minch, 2007d, 2007e] shows lenses of serpentinite outcropping along the Pine Rock Fault near the model profile. Below about 4 km, the dip of the Pine Rock Fault is unconstrained.

Along profile Z-Z', the SAF-CF junction is associated with two magnetic anomalies (labeled 4 and 5, Figure 6c). We suggest that these anomalies are produced by serpentinite within the San Andreas and Pine Rock fault zones, as well as by deformation of the Etchegoin Formation, which is weakly magnetic and crops out between the SAFZ and the fault contact with Great Valley sequence rocks [Dibblee and Minch, 2007d, 2007e]. The modeled thickness of the Etchegoin Formation varies across the junction in accordance with fault and fold patterns mapped at the surface [Dibblee and Minch, 2007d, 2007e].

Anomaly 6 (Figure 6c) is caused by strongly magnetic and dense ophiolitic rocks at the base of the Great Valley sequence that are folded up along the western limb of the Vallecitos syncline. Note that we interpret a 1 to 2 km thick slab of ophiolitic rocks extending beneath the Great Valley sequence, similar to model profiles X-X' and Y-Y' to the north. Profile Z-Z' is constrained by a well west of the SAFZ that bottoms in granite at 2200 feet (670 m). It should be noted that gravity control along profile Z-Z' is very poor, with an average station spacing of 5 km or greater along the profile (see Figure 3a).

5.2. Fault Intersection Model

The fault intersection model shown in Figure 7 is the result of integrated analysis of potential-field modeling, surface geologic mapping, and relocated seismicity described above. This fault model likely reflects multiple stages of complex fault deformation and reorganization in an inherently unstable Y-shaped junction. Slip appears to be transferred from the SAFZ to the CFZ on a series of buried cross faults, most of which are associated with slivers of serpentinite. Geophysical modeling and relocated seismicity show that the main trace of the San Andreas fault zone is clearly defined as a vertical to steeply southwest dipping structure between 5 and 10 km depth throughout the junction. South of Paicines, the Calaveras fault zone branches into two faults, the Pine Rock and Paicines Faults. Between Hollister and San Benito, modeling suggests that the CFZ is bounded by the northeast dipping Paicines and San Benito Faults, which form the southwest

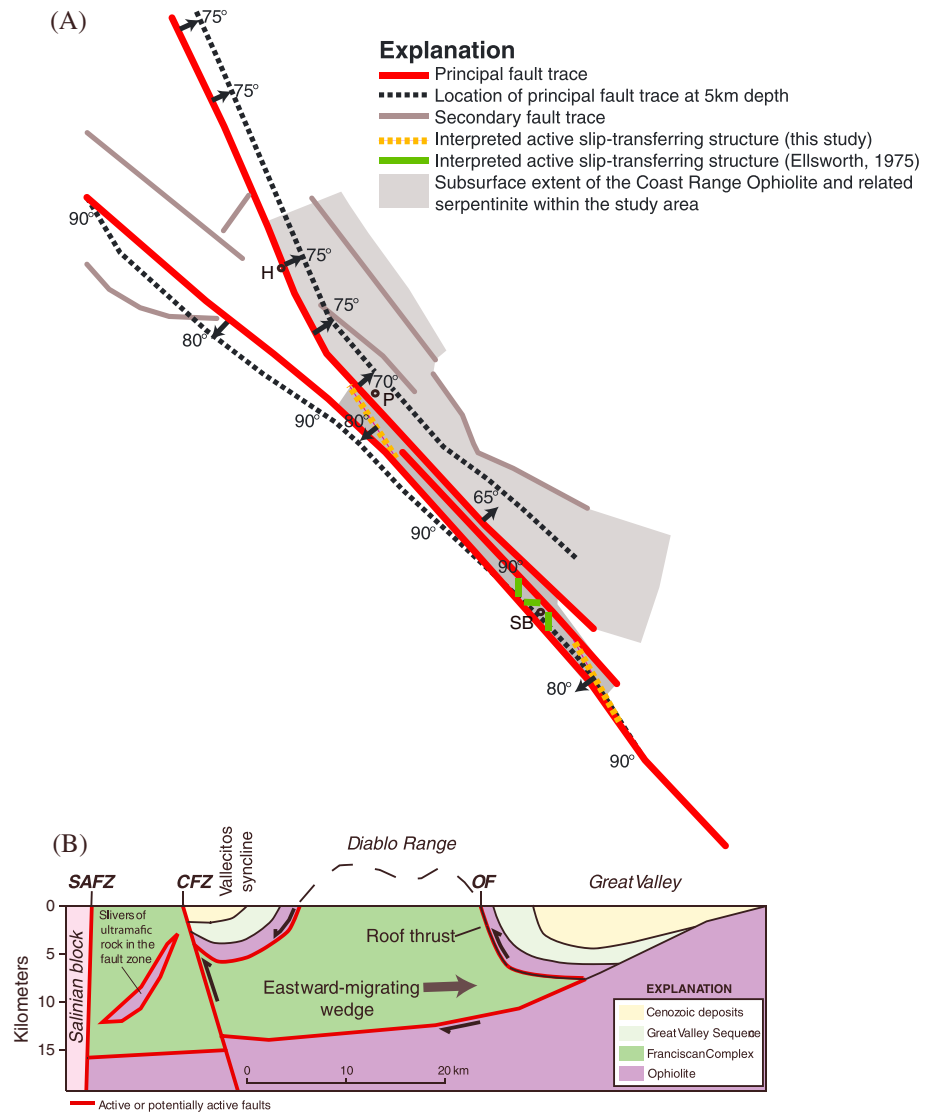


Figure 7. (a) Fault intersection model of the San Andreas-Calaveras fault junction. H, Hollister; P, Paicines; and SB, San Benito. (b) Schematic geologic cross section showing the deformed and reactivated roof thrust within the Vallecitos syncline. Red lines, active or potentially active faults; CFZ, Calaveras fault zone; OF, Ortigalita fault; SAFZ, San Andreas fault zone.

boundary of a strongly magnetic, folded slab of CRO within the Vallecitos syncline. South of San Benito, activity along the CFZ shifts from northeast dipping structures to the steeply southwest dipping Pine Rock Fault and related structures. This prominent change in fault zone geometry occurs where the Vallecitos syncline and associated CRO intersects the junction. During development of the SAF-CF junction, we suggest the CFZ may have preferentially followed a zone of weakness associated with frictionally weak lithologies (i.e., talc-bearing serpentinite) and/or fault structures separating the CRO from underlying Franciscan Complex.

While the SAFZ and CFZ are the main fault zones within the junction, both the Quien Sabe and Tres Pinos Faults are associated with a significant amount of seismicity and creep at depth [Templeton *et al.*, 2008], suggesting these structures are actively involved in deformation of the junction. The Quien Sabe Fault is associated with a 2 to 4 km wide zone of seismicity (Figure 5, profiles B-B' and C-C') that extends from 2 to 10 km depth, forming a near-vertical fault plane that appears to be offset to the southwest of the surface trace. North of profile B-B', the seismicity gradually shifts northeastward and is more in alignment with the surface trace. Bryant [1988] characterizes the Quien Sabe Fault as a Holocene active dextral strike-slip fault, dipping 70°E. Our results suggest that at least the seismically active portion of the Quien Sabe Fault is near vertical, rather than east dipping.

The Tres Pinos Fault is located between the Quien Sabe and Paicines Faults and is associated with a northeast dipping (75° – 80°) alignment of hypocenters that is only clearly visible along profile D-D' (Figure 5). Notably, there is a NS-trending alignment of seismicity visible in map view that appears to connect the Tres Pinos and Quien Sabe Faults (Figure 1). This seismicity lineament corresponds to the location of the 1986 magnitude 5.3 Tres Pinos earthquake and associated aftershocks (Figure 5). The focal mechanism of this earthquake indicates right-lateral strike-slip motion on a fault plane striking approximately NS and dipping 83° E [Simpson *et al.*, 1988], which is consistent with the strike of the lineament. This buried fault plane may represent a cross fault responsible for transferring slip between the Tres Pinos and Quien Sabe Faults within the junction.

5.3. Development of the Calaveras Fault Zone

The influence of preexisting crustal structure on the development of strike-slip fault systems is well documented globally [Christie-Blick and Biddle, 1985] and within California [e.g., Ponce *et al.*, 2003; Langenheim *et al.*, 2004]. Whether the preexisting structure provides a zone of weakness that promotes faulting or represents a barrier to faulting, that structure can significantly influence local faulting patterns. Combined geological and geophysical results suggest that the southern CFZ within the SAF-CF junction may have developed along a preexisting crustal structure associated with the CRO within the Vallecitos syncline.

East of the CFZ, we identify a laterally extensive, dense, magnetic body 1 to 8 km below the surface that we interpret as a folded 1 to 3 km thick tabular body of Coast Range Ophiolite at the base of the Great Valley sequence within the Vallecitos syncline. Potential-field modeling and relocated seismicity indicate that the southwestern edge of this magnetic body is defined by northeast dipping structures, including the Paicines and San Benito Faults. The intersection of the Vallecitos syncline with the San Benito Fault and the southern CFZ corresponds to a dramatic change in seismicity patterns and a prominent shift in active fault geometry suggesting the impingement of the Vallecitos syncline is currently influencing deformation patterns within the junction. Given that the Vallecitos syncline formed, or was forming, during initiation of the SAF-CF junction [Miller, 1998], it is conceivable that this structure was also significant in the early development of the junction.

Our results are most consistent with the thrust-wedge models [e.g., Wentworth *et al.*, 1984; McLaughlin *et al.*, 1988; Jayko *et al.*, 1987; Jachens *et al.*, 1995; Wakabayashi and Unruh, 1995] in which the CRO forms the basement of the Great Valley sequence and tectonic wedging associated with east vergent contraction resulted in the formation of low-angle roof thrusts that ultimately brought oceanic crust to the surface (Figure 7b). While we cannot rule out alternate models that implore primarily attenuation-related faulting as the primary mode of exhuming the CRO [e.g., Dickinson and Seely, 1979; Constenius *et al.*, 2000], only a low-angle roof thrust mechanism requires a relatively flat-lying section of oceanic crust at depth that is indicated in the geophysical data [Brocher *et al.*, 1994; Jachens *et al.*, 1995; Ponce *et al.*, 2003]. Since the earliest phases of tectonic wedging, which likely occurred during subduction, the CRO and related roof thrusts have likely been modified by multiple periods of structural reorganization, including extensional and transpressional deformation, and attenuation. The structure and serpentinization at the base of the CRO along the southwest limb of the Vallecitos syncline may reflect a relict roof thrust that has been folded and reactivated along the CFZ.

5.4. Fault Behavior

The presence of frictionally weak minerals, hydrothermal fluids, and high fluid pressures has been associated with weak fault zones and creep [e.g., Moore and Rymer, 2007; Lockner *et al.*, 2011; Fulton and Saffer, 2009]. Within the junction, the SAFZ and CFZ exhibit creep at the surface [Galehouse and Lienkaemper, 2003; Titus *et al.*, 2005] and at depth [Templeton *et al.*, 2008]. The Quien Sabe Fault also appears to creep at depth [Templeton *et al.*, 2008]. Serpentinized ultramafic rocks have been associated with a number of creeping faults in the San Francisco Bay region, including the San Andreas, Calaveras, and Hayward Faults [e.g., Ponce *et al.*, 2003, 2011; McPhee *et al.*, 2004; Graymer *et al.*, 2005; Moore and Rymer, 2007; Moore and Lockner, 2013]. Frictionally weak, talc-bearing serpentinite recovered from the active trace of the SAFZ at the San Andreas Fault Observatory at Depth drill site provided a link, albeit indirect, between serpentinite and creep along the SAFZ between San Juan Bautista and Cholame [Moore and Rymer, 2007].

Based on our findings, the distribution of serpentinite and related CRO is more widespread along the creeping section of the SAFZ and the southern CFZ than previously thought (Figure 7a), which reinforces the spatial correlation of serpentinite and creep presented by Moore and Rymer [2007]. Our work also provides

subsurface geophysical evidence that serpentinized ultramafic rocks along both the SAFZ and CFZ within the junction are consistently juxtaposed against Gabilan Range granites or other quartzofeldspathic rocks within the Franciscan Complex. Additionally, the geophysical characterization of northeast dipping structures within the SAF-CF junction, particularly along the CFZ, provides a mechanism for transporting hydrothermal fluids from depth into the fault junction. If talc-bearing serpentinite, quartzofeldspathic rocks, and hydrothermal fluids are prerequisites for creep in fault zones [Moore and Rymer, 2007; Moore and Lockner, 2013], then the widespread distribution of serpentinite and related CRO within the junction may help explain why both the SAFZ and CFZ creep.

5.5. Seismic Hazard Implications

Before discussing specific seismic hazard implications of this work, we evaluate the potential for earthquakes within the junction. The last decade has seen an increased interest in the dynamics and controls of rupture during large earthquakes, particularly in regard to multifault ruptures and ruptures along creeping faults. The recent occurrence of large ($M_w > 7$) earthquakes on creeping faults has led to a reevaluation of their potential seismic hazard. Recent studies by Noda and Lapusta [2013] and Harris and Abrahamsom [2014] show that earthquakes on creeping faults can be just as destructive as those that occur on locked faults. The San Andreas, Calaveras, and Quien Sabe Faults are known to creep within the junction, at least along portions of the faults [Galehouse and Lienkaemper, 2003; Johanson and Burgmann, 2005; Ryder and Burgmann, 2008; Templeton et al., 2008]. An important question is whether or not these faults are accumulating enough strain to produce damaging earthquakes. There is paleoseismic evidence that the nearby creeping Hayward Fault produces large earthquakes [Lienkaemper et al., 2010], including the magnitude 6.8 earthquake in 1868. While there is no unambiguous evidence of large earthquakes on faults within the junction, geodetic studies suggest the creeping SAF is accumulating strain that could be released in moderate to large earthquakes [Johanson and Burgmann, 2005; Ryder and Burgmann, 2008; Maurer and Johnson, 2014], as afterslip following events on nearby structures [Ryder and Burgmann, 2008], or that could sustain earthquakes propagating into the creeping section [Maurer and Johnson, 2014]. Notably, geodetic estimates of moment release and deficit are strongly influenced by both long-term slip rates [Maurer and Johnson, 2014] and fault geometry [Lindsey and Fialko, 2013].

Fault geometry and fault connectivity are important components of seismic hazard analysis because the three-dimensional geometry of faults affects the dynamics of fault rupture, slip, and ground motion [Oglesby et al., 2000]. Crustal deformation models involving vertical San Andreas and Calaveras Faults in the southern San Francisco Bay Area do not fit observations of fault-normal motion [Burgmann, 1997; Argus and Gordon, 2001] and argue for the existence of discrete detachment faults [Burgmann, 1997], a zone of distributed shearing on subhorizontal structures [Holbrook et al., 1996], or oblique slip on the southern Calaveras Fault [Burgmann, 1997]. Relocated seismicity and geophysical modeling suggest that the Paicines and San Benito Faults dip to the northeast at moderate to high angles, which is consistent with oblique slip. In addition, the fault separating the CRO from Franciscan basement at the base of the Vallecitos syncline could act as a discrete detachment surface, or serpentinized ultramafic rock could act as a zone of distributed shear. However, there is no clear evidence of such structures in the seismicity data. The dipping fault geometries presented in this study may help explain fault-normal motions currently observed in geodetic data and help constrain the seismic hazard.

The presence of connecting structures greatly influences the ability of an earthquake to propagate through a stepover [Oglesby, 2005], and therefore is important for assessing seismic hazard. In particular, the potential for ruptures to propagate from one fault to another to produce larger earthquakes is an important component of developing rupture models for seismic hazard analysis. Given the small surface separation between the SAF and CF in the junction, a through-going rupture is possible [Harris and Day, 1993, 1999], but the large slip rate difference between the two faults suggests that through-going ruptures have not occurred frequently [Schwartz et al., 2012]. We propose that the SAF and CF are, in fact, connected in the subsurface along steeply dipping cross faults, suggesting through-going ruptures are more likely than previously thought.

This study is just one of many along the San Andreas Fault System in which integrated geophysical investigations of three-dimensional fault geometry have revealed fault connectivity at depth where no

surface connection exists [e.g., Graymer *et al.*, 2007, Ponce *et al.*, 2004; Hardebeck, 2013]. We propose that the inherent instability of the SAF-CF junction and other similar Y junctions likely precludes the establishment of a long-term connection, while instead producing a chaotic damage zone, in which slip is distributed on a number of small cross faults that are active for only short periods of time. The ephemeral and distributed nature of such cross faults may also explain the absence of surface expression of these structures. Based on the identification of subsurface connecting structures within the SAF-CF junction, the possibility of a combined rupture should be evaluated in future seismic hazard studies, and the subsurface connectivity of other volumetric fault intersections should be properly evaluated.

6. Conclusions

Integrated analysis of potential-field, geologic, geodetic, and relocated seismicity data provides important information on the subsurface fault geometry, fault connectivity, and three-dimensional geologic framework of the SAF-CF junction. Geophysical evidence suggests that the San Andreas and Calaveras fault zones dip away from each other within the northern portion of the fault junction, bounding a triangular wedge of crust. This wedge changes shape to the south as the bounding fault geometries change and fault activity shifts between fault strands. Geophysical modeling and relocated seismicity show that the main trace of the San Andreas fault zone is clearly defined as a vertical to steeply southwest dipping structure between 5 and 10 km depth throughout the junction.

South of Paicines, the Paicines Fault merges with the San Benito Fault and this portion of the SAF-CF junction is characterized by a distinct wedge of seismicity that is bounded to the northeast by northeast dipping structures, including the San Benito Fault. The subsurface continuity of the active San Benito and Paicines Faults revealed in potential-field models and the associated relocated seismicity suggest that the San Benito Fault and related northeast dipping structures are part of the larger CFZ and should be considered in future hazard analyses. Potential-field modeling suggests the Paicines and San Benito Faults form the southwest boundary of a folded 1 to 3 km thick tabular body of CRO at the base of the Great Valley sequence within the Vallecitos syncline. The base of this magnetic slab, which is folded up along the Calaveras Fault, may represent a relict roof thrust formed by an eastward migrating wedge of Franciscan Complex. The intersection of the Vallecitos syncline with the San Benito Fault and the southern CFZ corresponds to a dramatic change in seismicity patterns and a prominent shift in active fault geometry suggesting that the impingement of the Vallecitos syncline is currently influencing deformation patterns within the junction, and may have influenced the early development of the junction as well. Fragments of CRO and related serpentinite caught up within the SAF-CF junction may facilitate slip transfer between structures that have limited or no connection at the surface. The abundance of serpentinite in the subsurface, either as fault-bounded slivers within the junction or as part of the broader stratigraphic sequence associated with the CRO, is a significant discovery that not only helps constrain the geometry of structures within the junction but may also help explain fault behavior and the tectonic evolution of the SAF-CF junction.

We identify two subsurface, steeply dipping, seismically active cross faults within the junction that currently connect and may transfer slip between the SAF and CF. The apparent ephemeral nature of these cross structures may explain why these two fault zones do not appear to connect at the surface. Based on the identification of subsurface connecting structures within the SAF-CF junction, a combined rupture should be considered in future seismic hazard studies, and the subsurface connectivity of other volumetric fault intersections should be thoroughly evaluated. The three-dimensional fault geometry and connectivity of the SAF-CF junction revealed in this study has implications for seismic hazards and may provide insight into the fault kinematics of other strike-slip fault intersections worldwide.

Acknowledgments

All geologic, gravity, aeromagnetic, geodetic, and relocated seismicity data used in this paper are published and publicly available (see citations provided in the Methods section). This work was supported by the National Cooperative Geologic Mapping, Earthquake Hazards, and Coastal and Marine Geology Programs of the U.S. Geological Survey. We acknowledge Pacific Gas and Electric Company for providing property access for the collection of gravity data. We thank Roland Bürgmann for his thoughtful comments and Jeanne Hardebeck, George Hillel, and Michael Oskin for providing constructive and thought-provoking reviews, which greatly improved this manuscript.

References

- Andrews, D. J. (1989), Mechanics of fault junctions, *J. Geophys. Res.*, *94*, 9389–9397, doi:10.1029/JB094iB07p09389.
- Argus, D. F., and R. G. Gordon (2001), Present tectonic motion across the Coast Ranges and San Andreas fault system in central California, *Geol. Soc. Am. Bull.*, *113*(12), 1580–1592.
- Bedrosian, P.A., M.J. Unsworth, and G. Egbert (2002), Magnetotelluric imaging of the creeping segment of the San Andreas Fault near Hollister, *Geophys. Res. Lett.*, *29*(11), 1506, doi:10.1029/2001GL014119.
- Blakely, R. J. (1995), *Potential Theory in Gravity and Magnetic Applications*, Cambridge Univ. Press, Cambridge, U. K.
- Blakely, R. J., and R. W. Simpson (1986), Approximating edges of source bodies from gravity or magnetic data, *Geophysics*, *51*, 1494–1498.

- Brocher, T. M., J. McCarthy, P. E. Hart, W. S. Holbrook, K. P. Furlong, T. V. McEvilly, J. A. Hole, and S. L. Klemperer (1994), Seismic evidence for a lower-crustal detachment beneath San Francisco Bay, California, *Science*, *265*, 1436–1439.
- Bryant, W. A. (Comp.) (1988), Fault number 64, Quien Sabe Fault, Quaternary fault and fold database of the United States, U.S. Geol. Surv. [Available at <http://earthquakes.usgs.gov/hazards/qfaults>, accessed 07/16/2014].
- Burford, R. O., and P. W. Harsh (1980), Slip on the San Andreas Fault in Central California from alignment array surveys, *Bull. Seismol. Soc. Am.*, *70*, 1233–1261.
- Burford, R. O., and J. C. Savage (1972), Tectonic evolution of a crustal wedge caught within a transform fault system, *Geol. Soc. Am. Abstr. Programs*, *4*(3), 134.
- Bürgmann, R. (1997), Active detachment faulting in the San Francisco Bay Area?, *Geology*, *25*(12), 1135–1138.
- Christie-Blick, N., and K. T. Biddle (1985), Deformation and basin formation along strike-slip faults, in *Strike-Slip Deformation, Basin Formation, and Sedimentation*, edited by K. T. Biddle and N. Christie-Blick, *Soc. Econ. Paleontol. Mineral. Spec. Publ.*, *37*, 1–34.
- Constenius, K. N., R. A. Johnson, W. R. Dickinson, and T. A. Williams (2000), Tectonic evolution of the Jurassic-Cretaceous Great Valley forearc, California: Implications for the Franciscan thrust-wedge hypothesis, *Geol. Soc. Am. Bull.*, *112*(11), 1703–1723.
- Cordell, L., and V. J. S. Grauch (1983), Mapping basement magnetization zones from aeromagnetic data in the San Juan Basin, New Mexico, *Geophysics*, *48*, 446.
- Dibblee, T. W. and J. A. Minch (2007a), Geologic map of the Bickmore Canyon quadrangle, Monterey and San Benito Counties, California, Dibblee Foundation Map DF-320, scale 1:24,000, Dibblee Geological Foundation.
- Dibblee, T. W., and J. A. Minch (2007b), Geologic map of the North Chalone Peak quadrangle, Monterey and San Benito Counties, California, Dibblee Foundation Map DF-303, scale 1:24,000, Dibblee Geological Foundation.
- Dibblee, T. W., and J. A. Minch (2007c), Geologic map of the Llanada quadrangle, San Benito County, California, Dibblee Foundation Map DF-318, scale 1:24,000, Dibblee Geological Foundation.
- Dibblee, T. W., and J. A. Minch (2007d), Geologic map of the Rock Spring Peak quadrangle, San Benito County, California, Dibblee Foundation Map DF-305, scale 1:24,000, Dibblee Geological Foundation.
- Dibblee, T. W., and J. A. Minch (2007e), Geologic map of the Topo Valley quadrangle, Monterey and San Benito Counties, California, Dibblee Foundation Map DF-304, scale 1:24,000, Dibblee Geological Foundation.
- Dickinson, W. R., and D. R. Seely (1979), Structure and stratigraphy of forearc regions, *Am. Soc. Pet. Geol. Bull.*, *63*, 2–31.
- Dickinson, W. R., C. A. Hopson, and J. B. Saleeby (1996), Alternate origins of the Coast Range Ophiolite (California): Introduction and implications, *Geol. Soc. Am. Today*, *6*(2), 1–10.
- Dorbath, C., D. Oppenheimer, F. Amelung, and G. King (1996), Seismic tomography and deformation modeling of the junction of the San Andreas and Calaveras Faults, *J. Geophys. Res.*, *101*, 27,917–27,941, doi:10.1029/96JB02092.
- Ellsworth, W. L. (1975), Bear Valley, California, earthquake sequence of February–March 1972, *Bull. Seismol. Soc. Am.*, *65*(2), 483–506.
- Feng, R., and T. V. McEvilly (1983), Interpretation of seismic reflection profiling data for the structure of the San Andreas fault zone, *Bull. Seismol. Soc. Am.*, *73*(6), 1701–1720.
- Fulton, P. M., and D. M. Saffer (2009), Potential role of mantle-derived fluids in weakening the San Andreas Fault, *J. Geophys. Res.*, *114*, B07408, doi:10.1029/2008JB006087.
- Galehouse, J. S., and J. J. Lienkaemper (2003), Inferences drawn from two decades of alignment array measurements of creep on faults in the San Francisco Bay region, *Bull. Seismol. Soc. Am.*, *93*(6), 2415–2433.
- Graymer, R. W., A. M. Sarna-Wojcicki, J. P. Walker, R. J. McLaughlin, and R. J. Fleck (2002), Controls on timing and amount of right-lateral offset on the East Bay fault system, San Francisco Bay region, California, *Geol. Soc. Am. Bull.*, *114*(12), 1471–1479.
- Graymer, R. W., D. A. Ponce, R. C. Jachens, R. W. Simpson, G. A. Phelps, and C. M. Wentworth (2005), Three-dimensional geologic map of the Hayward fault, Northern California: Correlation of rock units with variations in seismicity, creep rate, and fault dip, *Geology*, *33*(6), 521–524, doi:10.1130/G21435.1.
- Graymer, R. W., V. E. Langenheim, R. W. Simpson, R. C. Jachens, and D. A. Ponce (2007), Relatively simple through-going fault planes at large-earthquake depth may be concealed by the surface complexity of strike-slip faults, in *Tectonics of Strike-Slip Restraining and Releasing Basins*, edited by W. D. Cunningham and P. Mann, *Geol. Soc. London Spec. Publ.*, *290*, 189–201, doi:10.1144/SP290.5.
- Hardebeck, J. L. (2013), Geometry and earthquake potential of the Shoreline Fault, central California, *Bull. Seismol. Soc. Am.*, *103*(1), 447–462, doi:10.1785/0120120175.
- Hardebeck, J. L., A. J. Michael, and T. M. Brocher (2007), Seismic velocity structure and seismotectonics of the Eastern San Francisco Bay Region, California, *Bull. Seismol. Soc. Am.*, *97*(3), 826–842.
- Harris, R. A., and N. A. Abrahamson (2014), Strong ground motions generated by earthquakes on creeping faults, *Geophys. Res. Lett.*, *41*, doi:10.1002/2014GL060228.
- Harris, R. A., and S. M. Day (1993), Dynamics of fault interaction: Parallel strike-slip faults, *J. Geophys. Res.*, *98*, 4461–4472.
- Harris, R. A., and S. M. Day (1999), Dynamic 3D simulations of earthquakes on en echelon faults, *Geophys. Res. Lett.*, *26*(14), 2089–2092.
- Holbrook, W. S., T. M. Brocher, U. S. ten Brink, and J. A. Hole (1996), Crustal structure of a transform plate boundary: San Francisco Bay and the central California continental margin, *J. Geophys. Res.*, *101*, 22,311–22,334, doi:10.1029/96JB01642.
- Jachens, R. C., and A. Griscom (2004), Geophysical and geological setting of the earthquake, inferred from gravity and magnetic anomalies, in *The Loma Prieta, California, Earthquake of October 17, 1989 - Geologic Setting and Crustal Structure*, edited by R. E. Wells, *U.S. Geol. Surv. Prof. Pap.* 1550-E, E49–E80.
- Jachens, R. C., and M. L. Zoback (1999), The San Andreas fault in the San Francisco Bay Region, California: Structure and kinematics of a young plate boundary, *Int. Geol. Rev.*, *41*, 191–205.
- Jachens, R. C., A. Griscom, and C. W. Roberts (1995), Regional extent of Great Valley basement west of the Great Valley, California: Implications for extensive tectonic wedging in the California Coast Ranges, *J. Geophys. Res.*, *100*, 12,769–12,790, doi:10.1029/95JB00718.
- Jachens, R. C., C. M. Wentworth, and R. J. McLaughlin (1998), Pre-San Andreas location of the Gualala block inferred from magnetic and gravity anomalies, in *Geology and Tectonics of the Gualala Block, Northern California, Pacific Section, Book 84*, edited by W. P. Elder, pp. 27–64, Soc. of Econ. Paleontol. and Mineral. and Am. Assoc. of Pet. Geol., Los Angeles, Calif.
- Jachens, R. C., C. M. Wentworth, R. W. Graymer, J. P. Walker, F. C. Chuang, R. W. Simpson, and R. J. McLaughlin (2002), The Calaveras Fault, Northern California: A geophysical perspective on offset and 3-D geometry, *Eos Trans. AGU*, *83*(47), Fall Meet. Suppl., Abstract T71E-1205.
- Jayko, A. S., M. C. Blake, and T. Harms (1987), Attenuation of the Coast Range Ophiolite by extensional faulting, and nature of the Coast Range “Thrust”, California, *Tectonics*, *6*, 475–488, doi:10.1029/TC006i004p00475.
- Johanson, I. A., and R. Bürgmann (2005), Creep and quakes on the northern transition zone of the San Andreas Fault from GPS and InSAR data, *Geophys. Res. Lett.*, *32*, L14306, doi:10.1029/2005GL023150.

- Langenheim, V. E. (2014), Gravity, aeromagnetic and rock property data of the central California coast ranges, *U.S. Geol. Surv. Open-File Rep.* 2013-1282, 12 pp., doi:10.3133/ofr20131282.
- Langenheim, V. E., S. R. Stiles, R. C. Jachens, and E. B. Jewel (1997), Geometry of the San Andreas Fault inferred from gravity and magnetic data, south of Hollister, California, *Eos Trans. AGU*, 78, Fall Meet. Suppl., Abstract F454.
- Langenheim, V. E., R. C. Jachens, D. M. Morton, R. W. Kistler, and J. C. Matti (2004), Geophysical and isotopic mapping of preexisting crustal structures that influenced the location and development of the San Jacinto fault zone, Southern California, *Geol. Soc. Am. Bull.*, 116(9-10), 1143-1157, doi:10.1130/B25277.1.
- Lienkaemper, J. J., P. L. Williams, and T. P. Guilderson (2010), Evidence for a 12th large earthquake on the southern Hayward fault in the past 1900 years, *Bull. Seismol. Soc. Am.*, 100, 2024-2034.
- Lindsey, E. O., and Y. Fialko (2013), Geodetic slip rates in the southern San Andreas fault system: Effects of elastic heterogeneity and fault geometry, *J. Geophys. Res. Solid Earth*, 118, 689-697, doi:10.1029/2012JB009358.
- Lockner, D. A., C. Morrow, D. Moore, and S. Hickman (2011), Low strength of deep San Andreas Fault gauge from SAFOD core, *Nature*, 472, 82-85, doi:10.1038/nature09927.
- Loomis, K. B. (1990), Depositional environments and sedimentary history of the Etchegoin Group, West-central San Joaquin Valley, California, in *Structure, Stratigraphy, and Hydrocarbon Occurrences of the San Joaquin Basin, California: Bakersfield, Calif.*, edited by J. G. Kuespert and S. A. Reid, vol. 64, pp. 231-246, Society of Economic Paleontologists and Mineralogists and American Association of Petroleum Geologists, Pacific Section.
- Ludington, S., et al. (2007), Preliminary integrated geologic map databases for the United States-California, *U.S. Geol. Surv. Open-File Rep.* 2005-1305, 1.2, scale 1:750,000.
- Maurer, J., and K. Johnson (2014), Fault coupling and potential for earthquakes on the creeping section of the central San Andreas Fault, *J. Geophys. Res. Solid Earth*, 119, 4414-4428, doi:10.1002/2013JB010741.
- McLaughlin, R. J., C. D. Blome, and B. Murchev (1988), Tectonics of formation, translation, and dispersal of the Coast Range Ophiolite of California, *Tectonics*, 7, 1033-1056, doi:10.1029/TC007i005p01033.
- McLaughlin, R. J., W. V. Sliter, D. H. Sorg, P. C. Russell, and A. M. Sarna-Wojcicki (1996), Large-scale right-slip displacement on the East San Francisco Bay Region fault system, California: Implications for location of late Miocene to Pliocene Pacific plate boundary, *Tectonics*, 15, 1-18, doi:10.1029/95TC02347.
- McPhee, D. K., R. C. Jachens, and C. M. Wentworth (2004), Crustal structure across the San Andreas Fault at the SAFOD site from potential field and geologic studies, *Geophys. Res. Lett.*, 31, L12503, doi:10.1029/2003GL019363.
- Michael, A. J. (1988), Effects of three-dimensional velocity structure on the seismicity of the 1984 Morgan Hill, California, aftershock sequence, *Bull. Seismol. Soc. Am.*, 78(3), 1199-1221.
- Miller, D. D. (1998), Distributed shear, rotation, and partitioned strain along the San Andreas Fault, central California, *Geology*, 26(10), 867-870.
- Moore, D. E., and D. A. Lockner (2013), Chemical controls on fault behavior: Weakening of serpentinite sheared against quartz-bearing rocks and its significance for fault creep in the San Andreas system, *J. Geophys. Res. Solid Earth*, 118, 2558-2570, doi:10.1002/jgrb.50140.
- Moore, D. E., and M. J. Rymer (2007), Talc-bearing serpentinite and the creeping section of the San Andreas Fault, *Nature*, 448(16), 795-797, doi:10.1038/nature06064.
- Noda, H., and N. Lapusta (2013), Stable creeping fault segments can become destructive as a result of dynamic weakening, *Nature*, 493, 518-521, doi:10.1038/nature11703.
- Oglesby, D. D. (2005), The dynamics of strike-slip step-overs with linking dip-slip faults, *Bull. Seismol. Soc. Am.*, 95(5), 1604-1622, doi:10.1785/0120050058.
- Oglesby, D. D., R. J. Archuleta, and S. B. Nielsen (2000), Dynamics of dip-slip faulting: Explorations in two dimensions, *J. Geophys. Res.*, 105, 13,643-13,653, doi:10.1029/2000JB900055.
- Pavoni, N. (1973), A structural model for the San Andreas fault zone along the northeast side of the Gabilan Range, in *Proceedings of the Conference on Tectonic Problems of the San Andreas Fault System*, Univ. Ser. Geol. Sci., vol. 13, pp. 259-267, Stanford Univ. Press, Stanford, Calif.
- Perkins, J. A. (1987), Provenance of the upper Miocene and Pliocene Etchegoin Formation: Implications for paleogeography of the late Miocene of central California, *U.S. Geol. Surv. Open-File Rep.* 87-167, 93 pp.
- Phelps, G. A., R. W. Graymer, R. C. Jachens, D. A. Ponce, R. W. Simpson, and C. M. Wentworth (2008), Three-dimensional geologic map of the Hayward Fault zone, San Francisco Bay Region, California, *U.S. Geol. Surv. Sci. Invest. Map 3045*. [Available at <http://pubs.usgs.gov/sim/3045/>]
- Ponce, D. A., T. G. Hildenbrand, and R. C. Jachens (2003), Gravity and magnetic expression of the San Leandro Gabbro with implications for the geometry and evolution of the Hayward fault zone, Northern California, *Bull. Seismol. Soc. Am.*, 93(1), 1-13.
- Ponce, D. A., R. W. Simpson, R. W. Graymer, and R. C. Jachens (2004), Gravity, magnetic, and seismicity profiles suggest a connection between the Hayward and Calaveras Faults, Northern California, *Geochem. Geophys. Geosyst.*, 5, Q07004, doi:10.1029/2003GC000684.
- Ponce, D. A., R. W. Graymer, R. C. Jachens, and R. W. Simpson (2011), In search of segment boundaries along the Hayward fault and implications on earthquake hazards, in *Proceedings of the Third Conference on Earthquake Hazards in the Eastern San Francisco Bay Area—Science, Hazard, Engineering and Risk*, Calif. Geol. Surv. Spec. Rep. 219, edited by K. Knudsen et al., pp. 77-92, Sacramento, Calif.
- Robbins, S. L. (1982), Complete bouguer gravity, aeromagnetic, and generalized geologic map of the Hollister 15-minute quadrangle, California, *U.S. Geol. Surv. Geophys. Invest. Map*, GP-945, scale 1:62,500.
- Roberts, C. W., and R. C. Jachens (1999), Preliminary aeromagnetic anomaly map of California *U.S. Geol. Surv. Open-File Rep.* 99-440, 14 pp.
- Rogers, T. H. (1993), Geology of the Hollister and San Felipe quadrangle, San Benito, Santa Clara, and Monterey counties, California, *Cal. Div. Mines and Geol. Open-File Rep.* 93-01, scale 1:24,000.
- Ryder, I., and R. Bürgmann (2008), Spatial variations in slip deficit on the central San Andreas Fault from InSAR, *Geophys. J. Int.*, 175, 837-852.
- Saltus, R. W., and R. J. Blakely (2011), Unique geologic insights from "non-unique" gravity and magnetic interpretation, *GSA Today*, 21(12), 4-11, doi:10.1130/G136A.1.
- Schaff, D. P., G. H. R. Bokelmann, G. C. Beroza, F. Waldhauser, and W. L. Ellsworth (2002), High-resolution image of the Calaveras Fault seismicity, *J. Geophys. Res.*, 107(B9), 2186, doi:10.1029/2001JB000633.
- Schwartz, D. P., P. J. Haeussler, G. G. Seitz, and T. E. Dawson (2012), Why the 2002 Denali Fault rupture propagated onto the Totschunda Fault: Implications for fault branching and seismic hazards, *J. Geophys. Res.*, 117, B11304, doi:10.1029/2011JB008918.
- Simpson, R. W., R. W. Jachens, R. C. Saltus, and R. J. Blakely (1986), Isostatic residual gravity, topographic, and first-vertical derivative gravity maps of the conterminous United States, *U.S. Geol. Surv. Geophys. Invest. Map 975*, 2 plates.
- Simpson, R. W., S. S. Schulz, L. D. Dietz, and R. O. Burford (1988), The response of creeping parts of the San Andreas Fault to earthquake on nearby faults: Two examples, *Pure Appl. Geophys.*, 126(2-4), 665-685.
- Simpson, R. W., R. W. Graymer, R. C. Jachens, D. A. Ponce, and C. M. Wentworth (2003), Structures in the Hayward and Calaveras fault zones from relocated seismicity, *Eos Trans. AGU*, 84(47), Fall Meet. Suppl., Abstract T11D-0426.

- Templeton, D. C., R. M. Nadeau, and R. Bürgmann (2001), Structure and kinematics at the juncture between the San Andreas and Southern Calaveras Faults, *Eos Trans. AGU*, 82(47), Fall Meet. Suppl., Abstract S32E-02.
- Templeton, D. C., R. M. Nadeau, and R. Bürgmann (2008), Behavior of repeating earthquake sequences in central California and the implications for subsurface fault creep, *Bull. Seismol. Soc. Am.*, 98(1), 52–65, doi:10.1785/0120070026.
- Thurber, C., S. Roecker, W. Ellsworth, Y. Chen, W. Lutter, and R. Sessions (1997), Two-dimensional seismic image of the San Andreas Fault in the Northern Gabilan Range, central California: Evidence for fluids in the fault zone, *Geophys. Res. Lett.*, 24, 1591–1594, doi:10.1029/97GL01435.
- Titus, S. J., C. DeMets, and B. Tikoff (2005), New slip rate estimates for the creeping segment of the San Andreas Fault, California, *Geology*, 33(3), 205–208, doi:10.1130/G21107.1.
- U.S. Geological Survey and California Geological Survey (2006), Quaternary fault and fold database for the United States. [Available from U.S. Geological Survey <http://earthquake.usgs.gov/hazards/qfaults/download.php>, accessed 10/15/2012.]
- Wagner, D. L., H. G. Greene, G. J. Saucedo, and C. L. Pridmore (2002), Geologic map of the Monterey 30' × 60' quadrangle and adjacent areas, California, *Calif. Geol. Surv., Reg. Geol. Map 1*, scale 1:100,000.
- Wakabayashi, J. (1999), Distribution of displacement on and evolution of a young transform fault system: The northern San Andreas fault system, California, *Tectonics*, 18, 1245–1274, doi:10.1029/1999TC900049.
- Wakabayashi, J., and J. R. Unruh (1995), Tectonic wedging, blueschist metamorphism, and exposure of blueschists: Are they compatible?, *Geology*, 23(1), 85–88.
- Waldhauser, F., and W. L. Ellsworth (2000), A double-difference earthquake location algorithm, method and application to the northern Hayward Fault, *Bull. Seismol. Soc. Am.*, 90, 1353–1368.
- Waldhauser, F., and W. L. Ellsworth (2002), Fault structure and mechanics of the Hayward Fault, California, from double-difference earthquake locations, *J. Geophys. Res.*, 107(B3), 2054, doi:10.1029/2000JB000084.
- Waldhauser, F., and D. P. Schaff (2008), Large-scale relocation of two decades of Northern California seismicity using cross-correlation and double-difference methods, *J. Geophys. Res.*, 113, B08311, doi:10.1029/2007JB005479.
- Wang, C., F. Rui, Y. Zhengsheng, and S. Xingjue (1986), Gravity anomaly and density structure of the San Andreas fault zone, *Pure Appl. Geophys.*, 124(1/2), 127–140.
- Watt, J. T., R. W. Graymer, R. W. Simpson, D. A. Ponce, R. C. Jachens, G. A. Phelps, and C. M. Wentworth (2007), A three-dimensional geologic model of the Hayward-Calaveras fault junction, *Eos Trans. AGU*, 88(52), Fall Meet. Suppl., Abstract S21A-0238.
- Watt, J. T., D. A. Ponce, R. W. Graymer, R. W. Simpson, R. C. Jachens, and C. M. Wentworth (2011), The Mt. Lewis fault zone: Tectonic implications for eastern San Francisco Bay Area, in *Proceedings of the Third Conference on Earthquake Hazards in the Eastern San Francisco Bay Area—Science, Hazard, Engineering and Risk*, edited by K. Knudsen, pp. 313–322, *Calif. Geol. Surv. Spec. Rep.*, 219, Sacramento, Calif.
- Wentworth, C. M., M. C. Blake Jr., D. L. Jones, A. W. Walter, and M. D. Zoback (1984), Tectonic wedging associated with emplacement of the Franciscan assemblage, California Coast Ranges, in *Franciscan Geology of Northern California*, vol. 43, edited by M. C. Blake Jr., pp. 163–173, Society of Economic Paleontologists and Mineralogists, Pacific Section.
- Zoback, M. L., R. C. Jachens, and J. A. Olson (1999), Abrupt along-strike change in tectonic style: San Andreas Fault zone, San Francisco Peninsula, *J. Geophys. Res.*, 104, 10,719–10,742, doi:10.1029/1998JB900059.